



**The Abdus Salam
International Centre for Theoretical Physics**



2015-16

**Joint ICTP/IAEA Workshop on Advanced Simulation and Modelling
for Ion Beam Analysis**

23 - 27 February 2009

Manual analysis: When software is useless

N.P. Barradas
*Instituto Tecnológico e Nuclear
Portugal*



Joint ICTP/IAEA Workshop on Advanced Simulation and
Modelling for Ion Beam Analysis, 23-27 February 2009

Manual analysis: When software is useless

Nuno P. Barradas (nunoni@itn.pt)

Instituto Tecnológico e Nuclear



Overview

- Introduction
- Example 1: Comparison of simulations with data not accurate
- Example 2: Models not good enough
- Example 3: Data highly ambiguous
- Conclusions



Why is software useful?

- Efficient way of doing many repetitive calculations
 - Direct comparison of simulation with data
 - Automated fitting
- Easy access to data bases (stopping, cross sections)
- Integration of advanced physical models
- Recognise when data is insufficient or ambiguous
- Help design experiments
- Education
- **Many more !!!**



So when is it not useful?

- Direct comparison of simulation with data; automated fitting
 - May not be accurate enough!
- Easy access to data bases (stopping, cross sections)
- Integration of advanced physical models
 - If reality (beam/sample interaction or sample description) is not well modelled, or data bases are wrong, good simulations are wrong
- Recognise when data is insufficient or ambiguous
 - Sometimes no further data can be obtained, and still results are needed



Example 1:

RBS study of thin oxide layers prepared by reactive magnetron sputtering

N.P. Barradas, J.C. Soares

CFNUL (Lisbon University), Portugal

M.F. da Silva

ITN, Sacavém, Portugal

T.S. Plaskett and P.P. Freitas

INESC, Lisbon, Portugal

Overview

Introduction

Experimental details

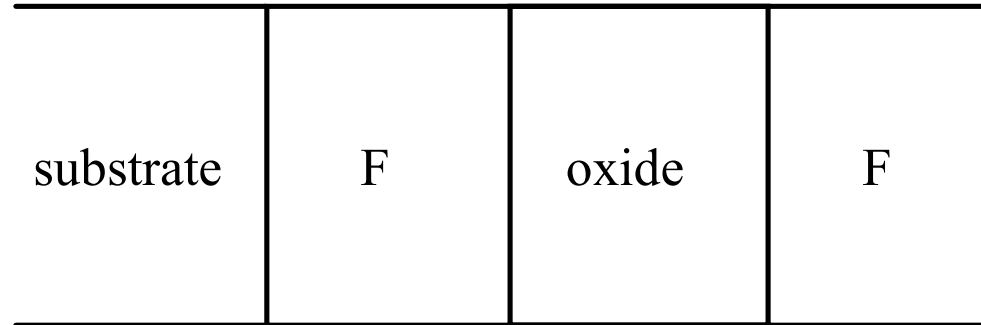
Results

Conclusions



Introduction

- Ferromagnetic/oxide/ferromagnetic junctions:



- Electron tunneling through the insulator oxide
 - Related magnetoresistance could be used in devices
 - The structure of the system affects its properties:
 - Oxide formation at the interfaces
 - Layer thickness
 - Layer composition
 - This work:
 - Si / NiFe 60Å / Al₂O₃ t / Co 65Å $t \in [0, 200 \text{ Å}]$
 - Si / NiFe 60Å / MgO t / Co 65Å $t \in [0, 160 \text{ Å}]$
- Aim: determine the oxygen content of each layer.



Sample preparation

- Magnetron sputtering:
 - Pbase = 1×10^{-7} Torr
 - Ni₈₁Fe₁₉, Co: 1 Å/s in Ar atmosphere
 - Oxide layers: from Al or Mg metallic targets, 0.1 to 0.2 Å/s in 1.5 mTorr Ar-10 vol% O₂ atmosphere
- Deposition process:
 - NiFe is deposited on the Si wafer
 - O₂ is introduced in the chamber
 - Al or Mg is deposited
 - O₂ is removed
 - Co cap layer is deposited

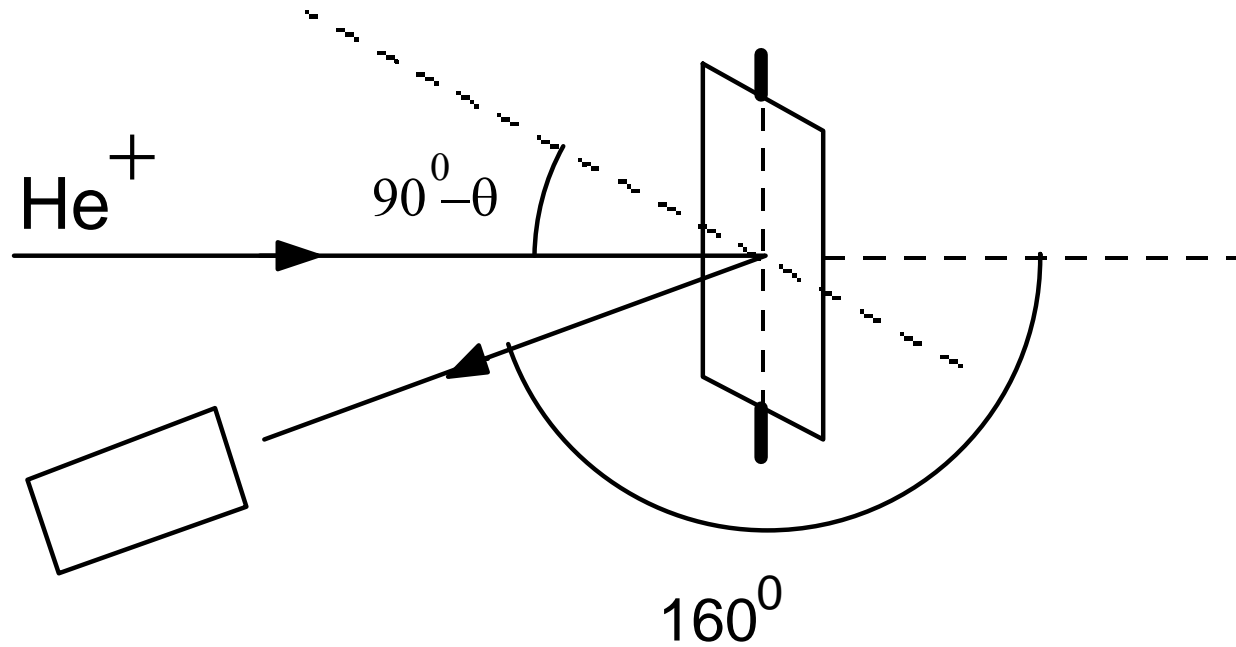
Vacuum is never broken during the process
In samples with $t=0$ Å, no O₂ is introduced



RBS

- 1.0 MeV He⁺

- Cornell geometry:



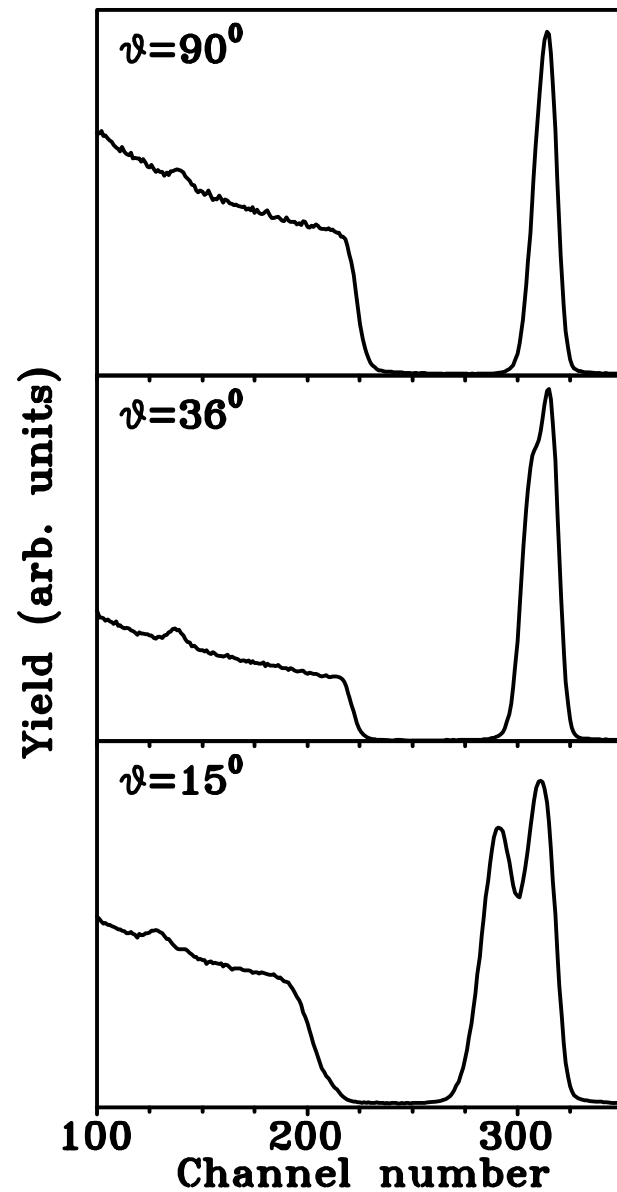
- Tilt angles used:

Al₂O₃: 90°, 45°, 36°, 15°

MgO: 90°, 45°, 36°, 20°



● Si / NiFe 60Å / Al₂O₃ 25Å / Co 65Å



125 Å depth resolution

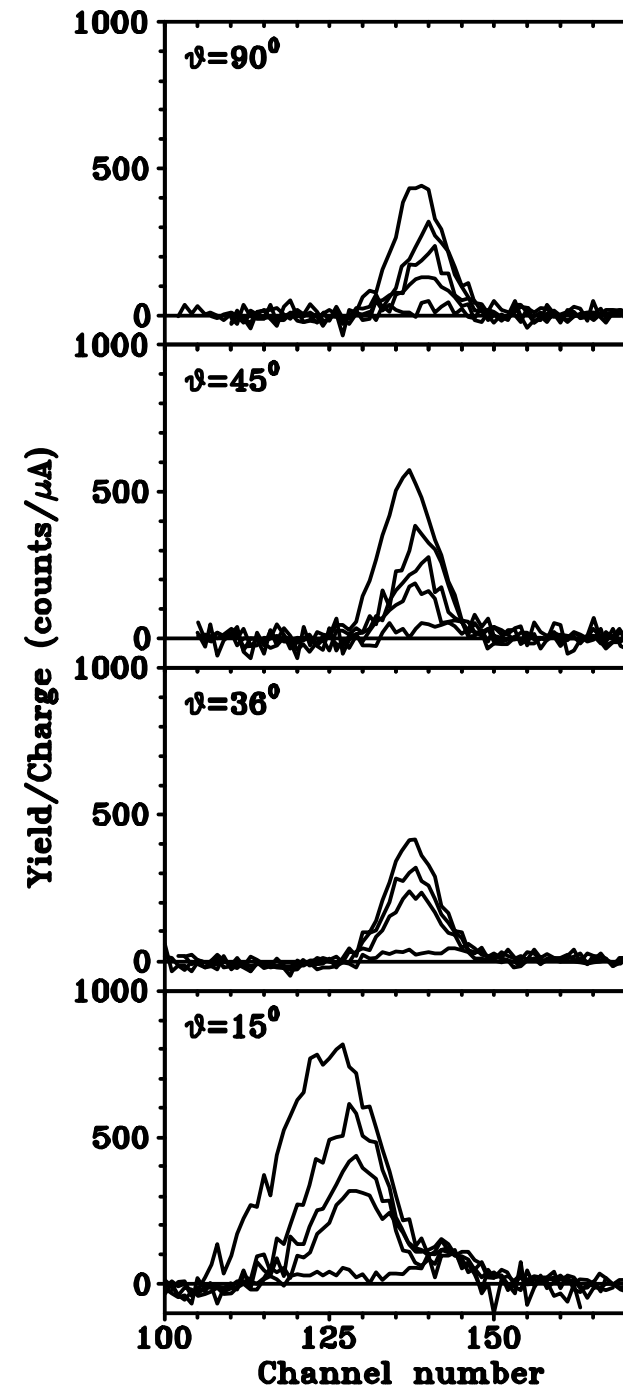
Channeling: reduced background

33 Å depth resolution



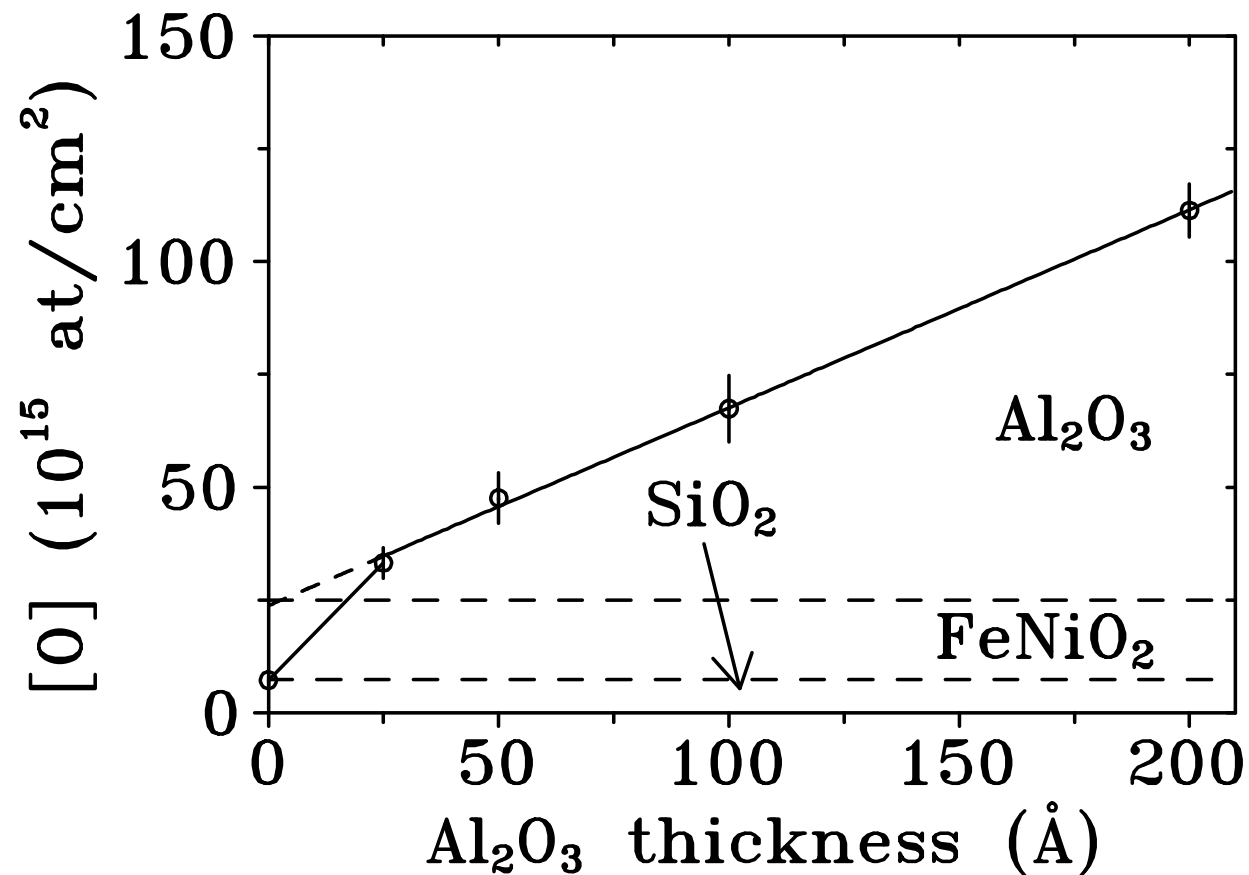
● Si / NiFe 60Å / Al₂O₃ t / Co 65Å

- Larger Al₂O₃ thickness \Rightarrow larger oxygen peak
- At $t=0$ Å there is still oxygen:
Si native oxide, Co surface oxide
- At 15° these contributions are separated





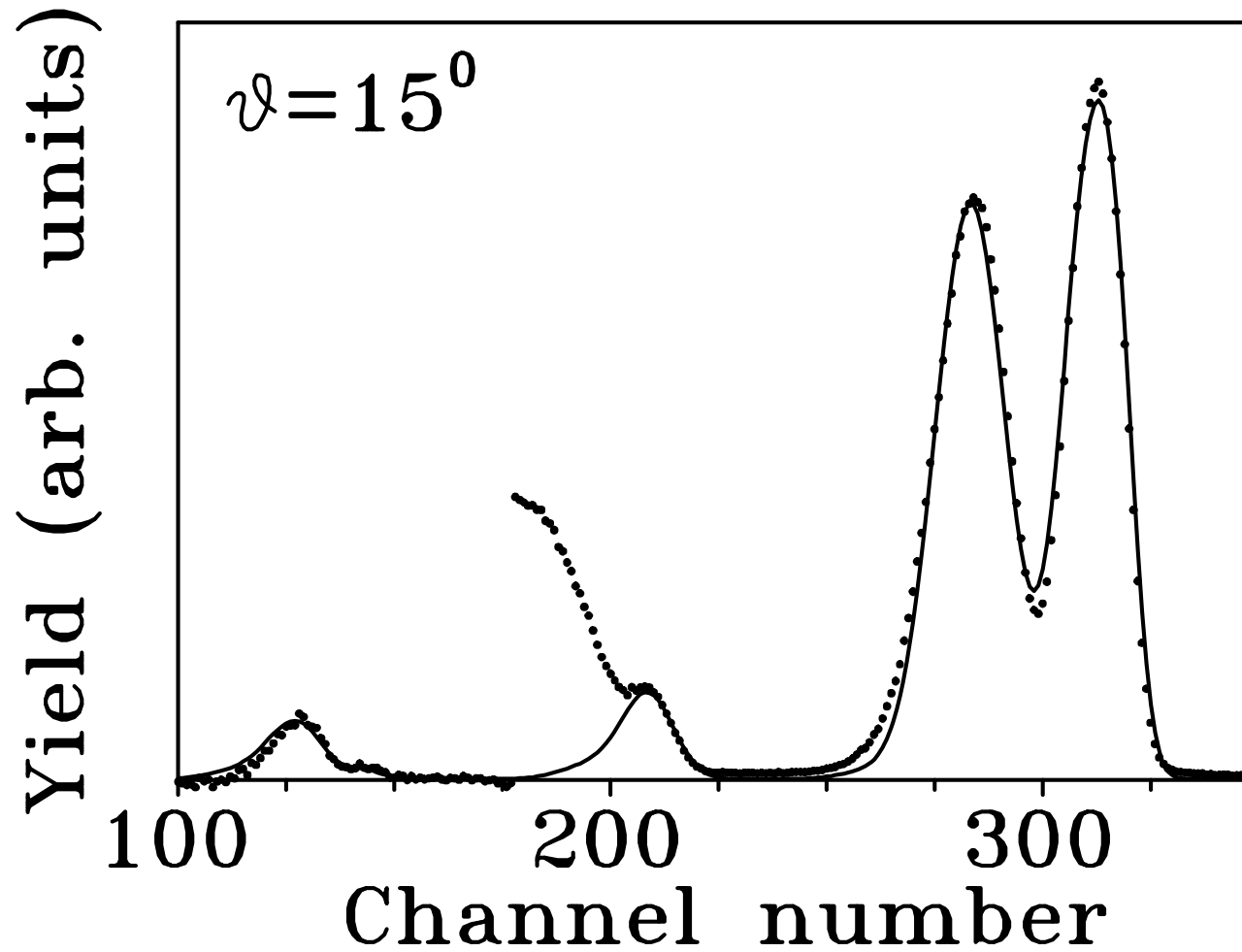
● Si / NiFe 60Å / Al₂O₃ t / Co 65Å



- $t = 0$ Å: Si native oxide thickness is 24(4) Å
- $t \geq 25$ Å: [O] is proportional to $t \Rightarrow \text{Al}_2\text{O}_{2.7(6)}$
- Excess oxygen \Rightarrow extra oxide layer: NiFe 18(6) Å



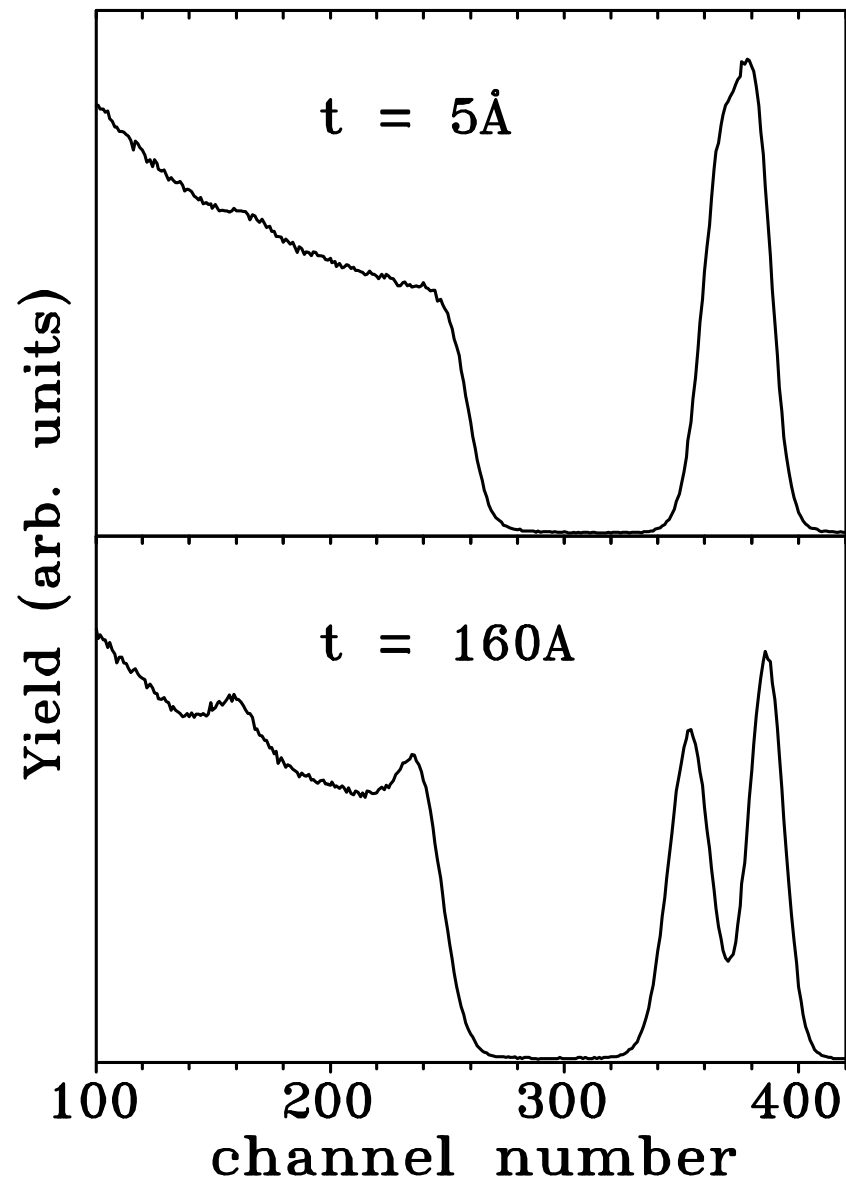
● Si / NiFe 60Å / Al₂O₃ t / Co 65Å



- No further fitting: good agreement.

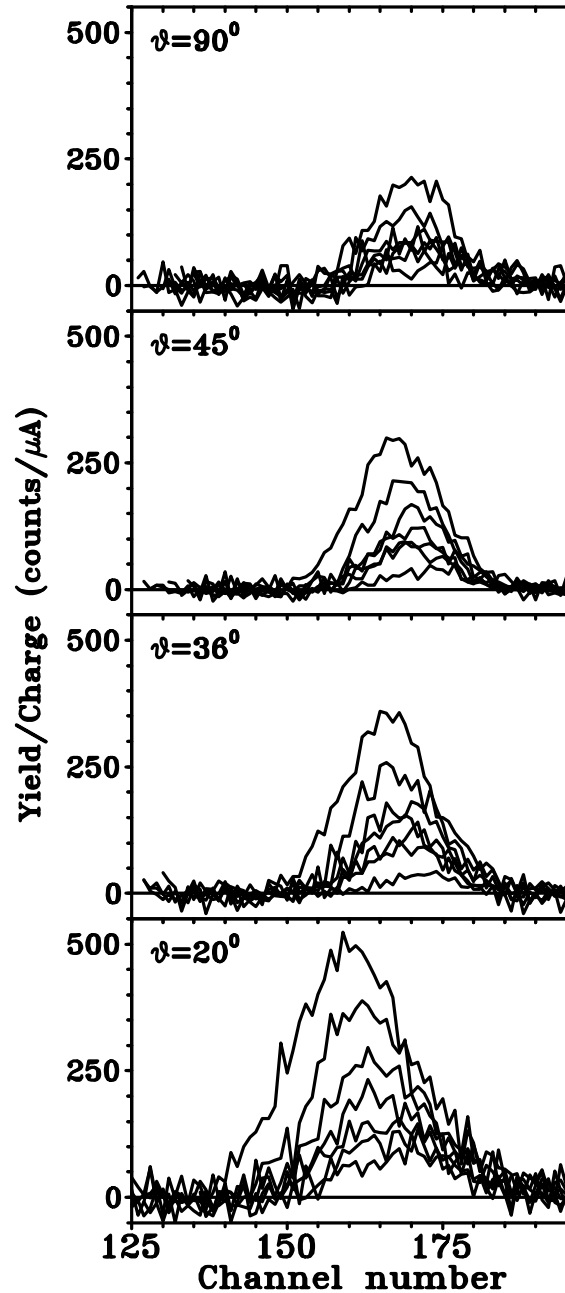


● Si / NiFe 60Å / MgO t / Co 65Å
 $t = 0, 5, 10, 20, 40, 80, 160 \text{ \AA}$





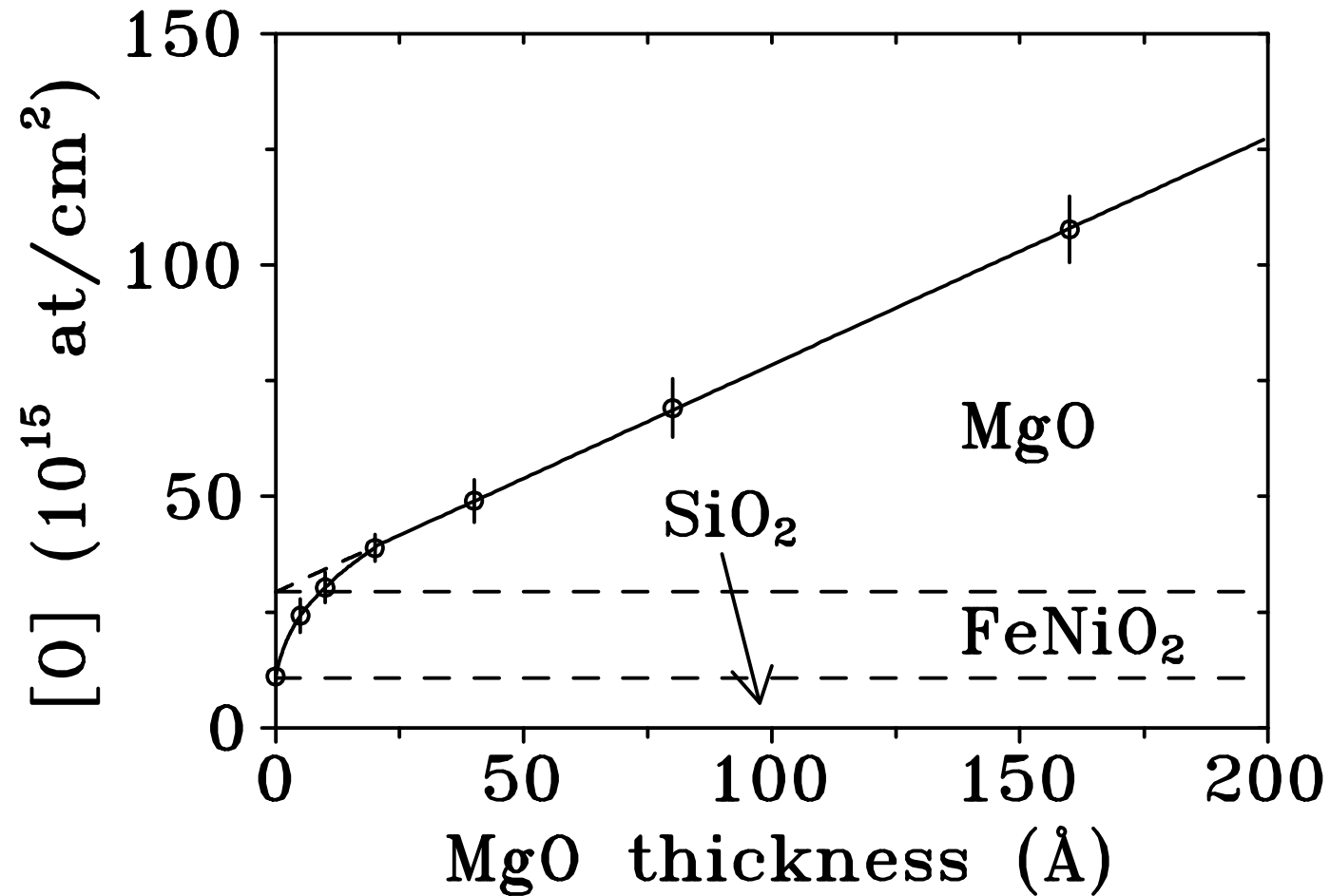
● Si / NiFe 60Å / MgO t / Co 65Å



- Larger MgO thickness \Rightarrow larger oxygen peak
- At $t=0$ Å there is still oxygen:
Si native oxide, Co surface oxide



● Si / NiFe 60Å / MgO t / Co 65Å



- $t = 0$ Å: Si native oxide thickness is 36(6) Å
- $t \geq 20$ Å: $[O]$ is proportional to $t \Rightarrow MgO_{1.3(4)}$
- Excess oxygen \Rightarrow extra oxide layer: NiFe 19(4) Å
- Transition regime between $t = 0$ and 20 Å



Example 2:

Grazing angle RBS analysis of
 $\text{Si/Re } 50 \text{ \AA}/(\text{Co } 20\text{\AA}/\text{Re } 5\text{\AA})_{16}$



Sample:

Si/Re 50 Å/(Co 20Å/Re 5Å)₁₆

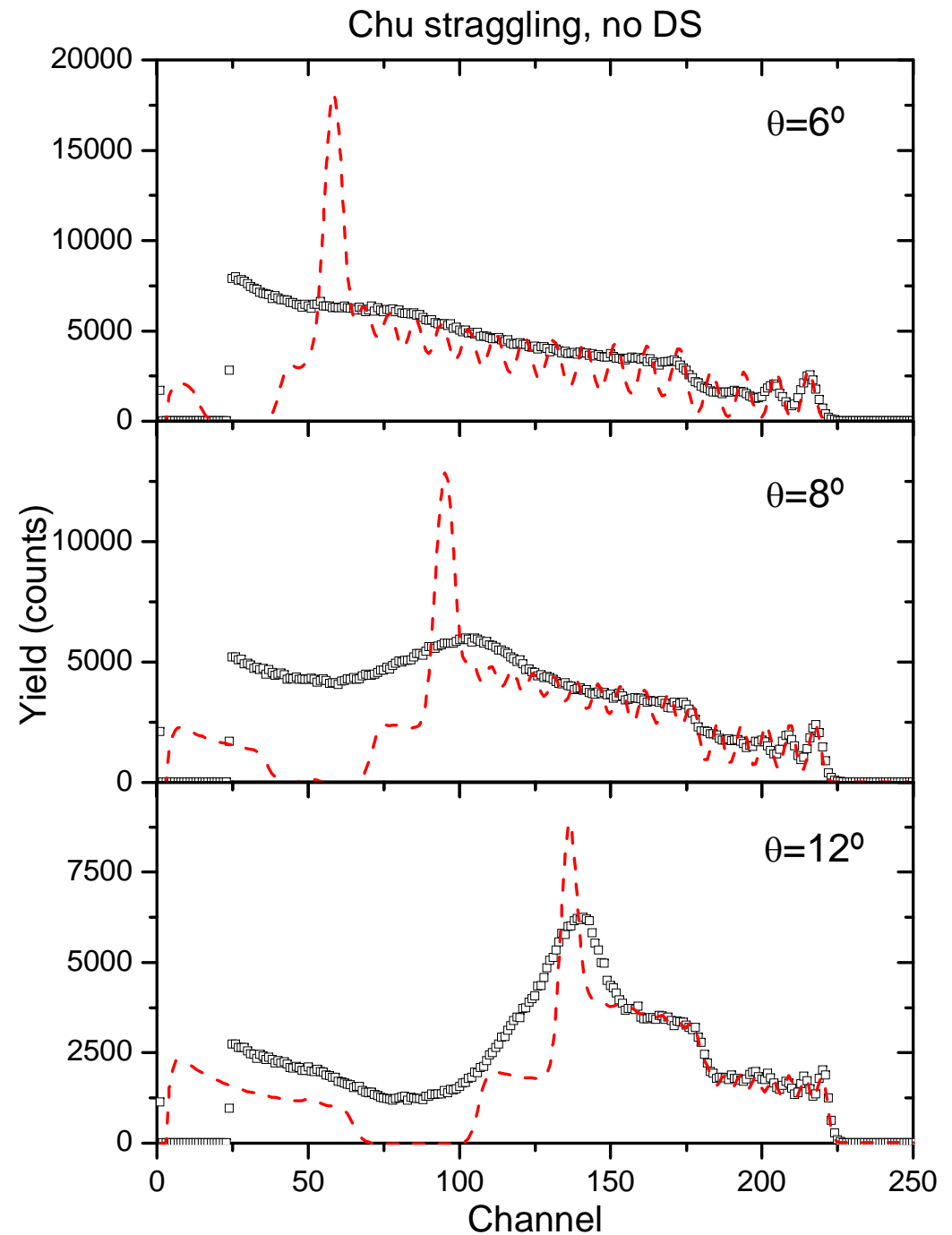
1 MeV He⁺ beam detected at
160° in the Cornell geometry

Grazing angle: down to 6° with
surface of the sample

Bohr+Chu straggling:

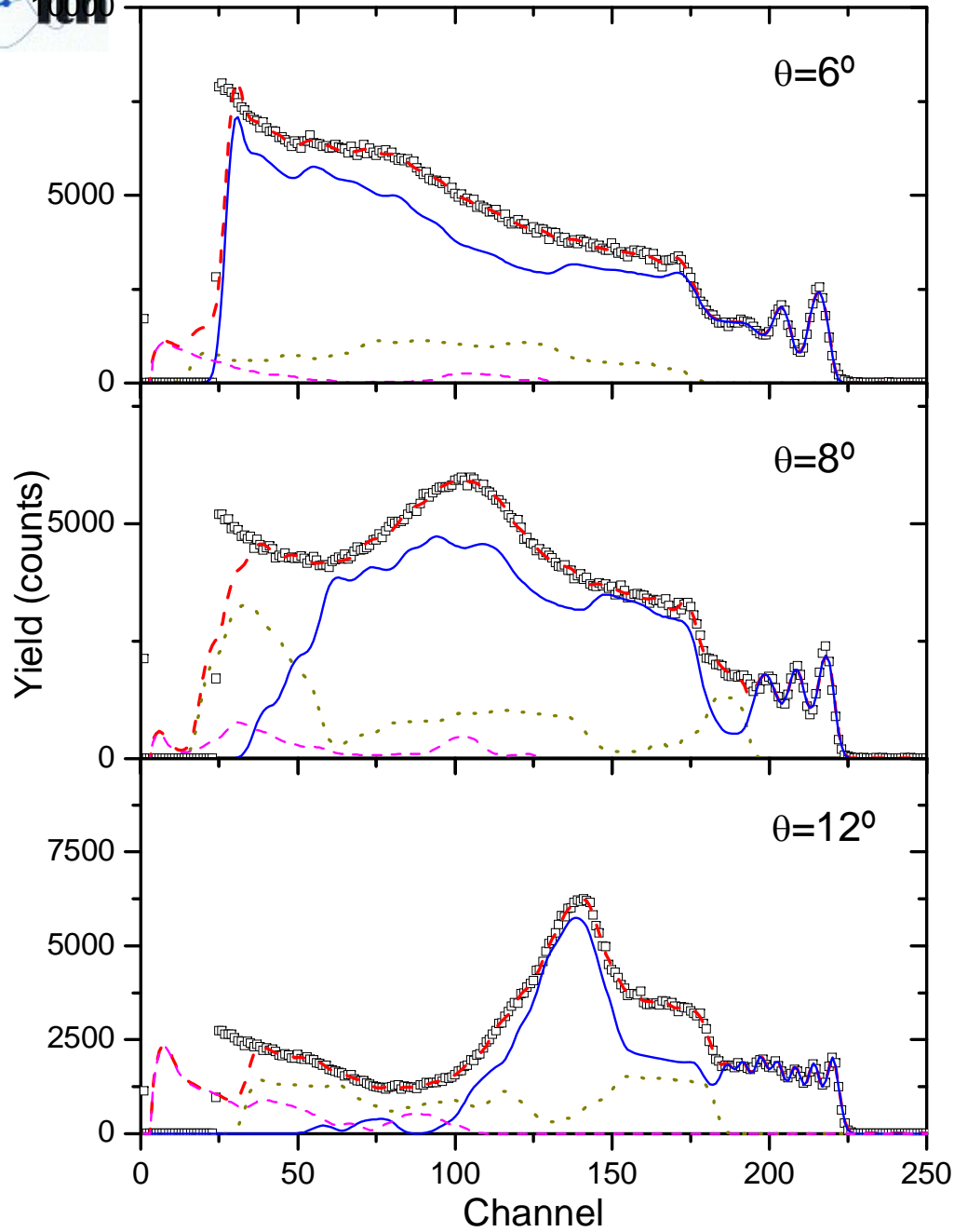
Bad simulation for nominal
structure

Impossible to fit all spectra with
the same profile



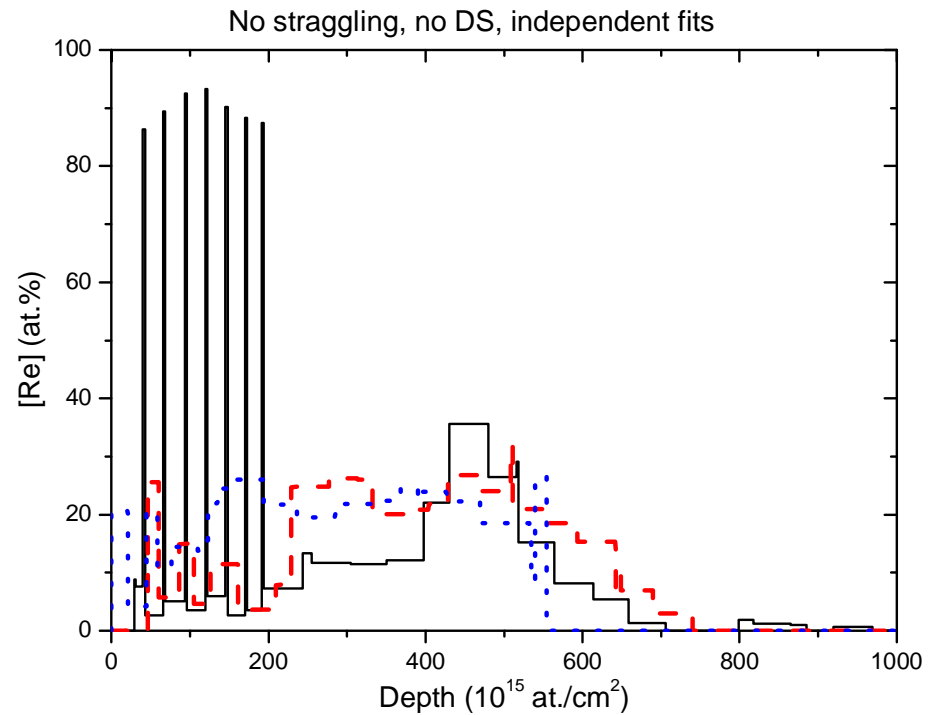


Chu straggling, no DS, independent fits



Fit the spectra one by one:

Perfect fits with no meaning

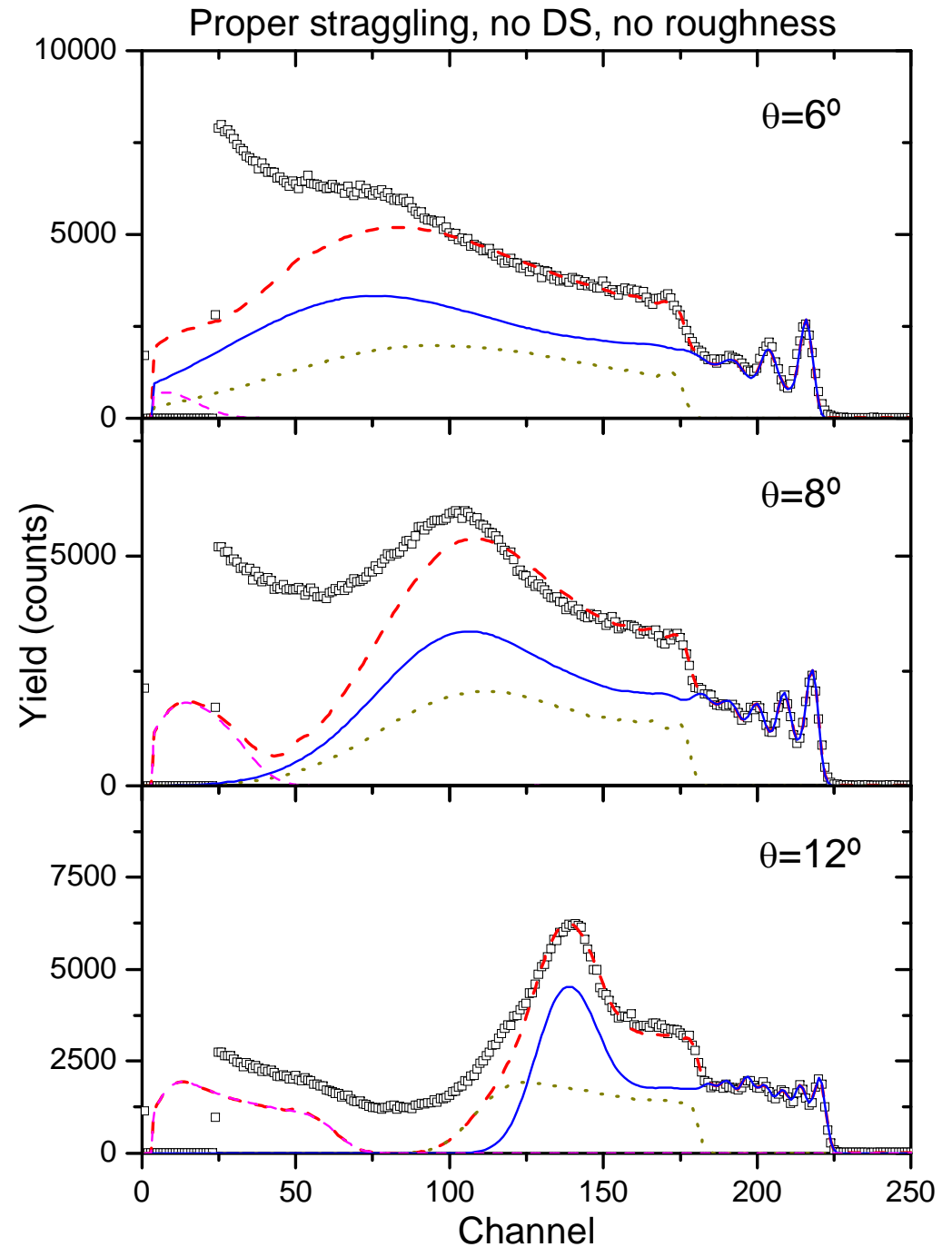




No DS: poor simulation at low energy (no problem!)

No roughness: simulation requires Co/Re diffusion:

TEM shows interfaces are sharp but not flat!

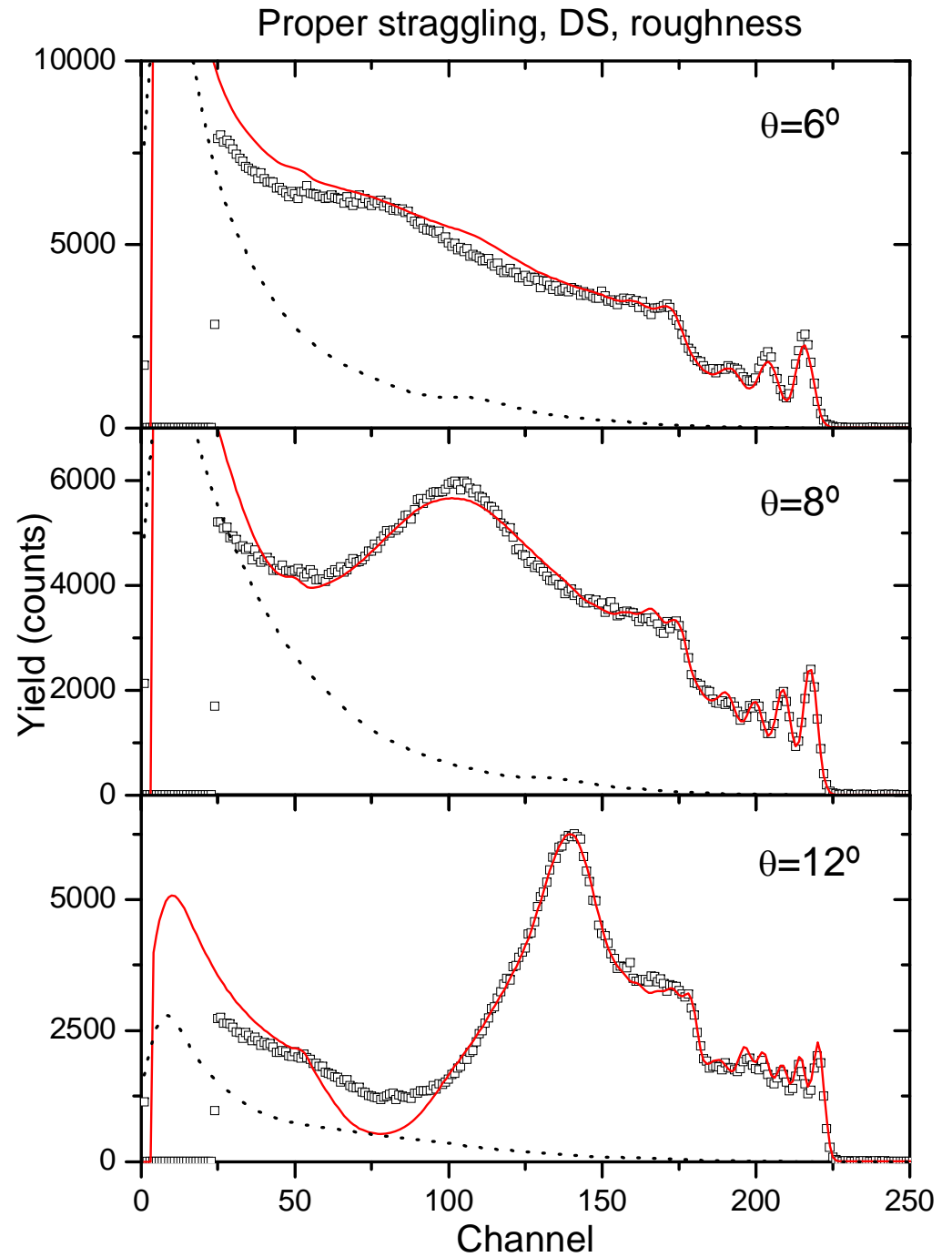




Best analytic simulation
available:

Pretty good, but not perfect

A fit would lead to a wrong
depth profile





Example 3:

RBS analysis of InGaN/GaN quantum wells for hybrid structures with efficient Förster coupling

N. P. Barradas (nunoni@itn.pt)

E. Alves, S. Pereira, I. M. Watson

Overview

Introduction

Experimental details

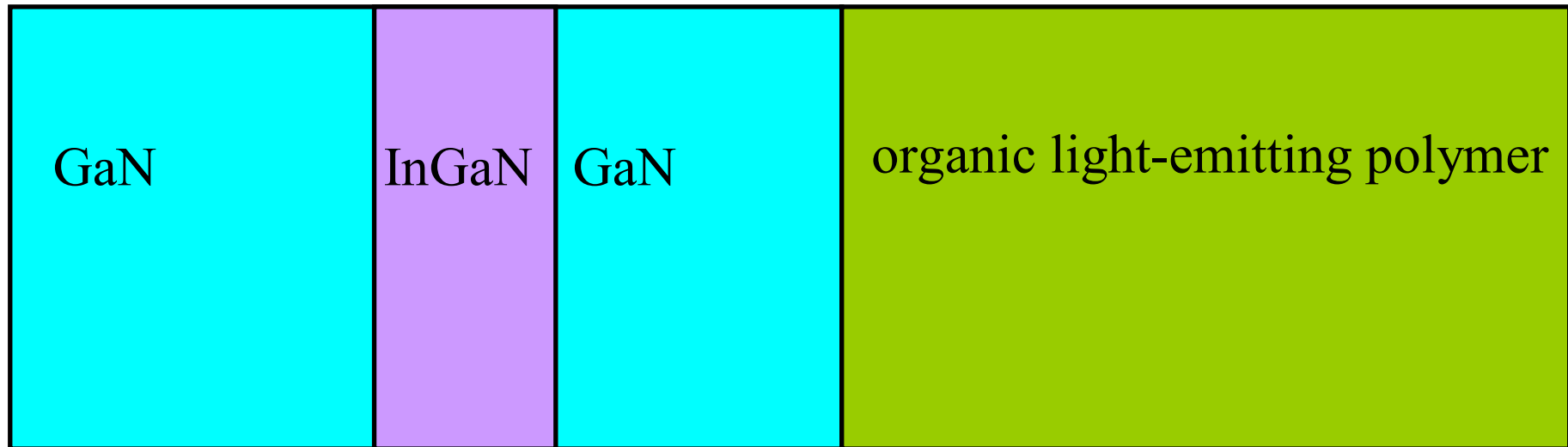
RBS analysis

Förster coupling



Förster resonant energy transfer (FRET)

substrate $\approx 2\text{nm}$ $< 10\text{nm}$



semiconductor QW: donor

excellent electrical properties

complex and costly

near-UV to the green visible

LEP: acceptor

cheap, high throughput

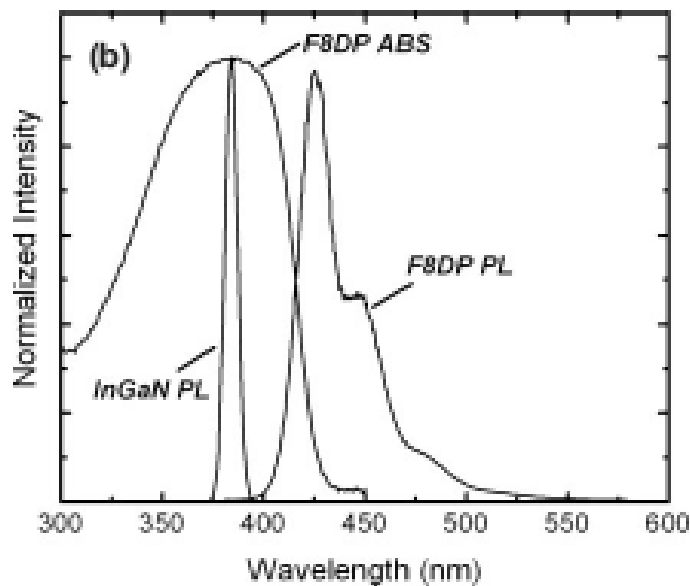
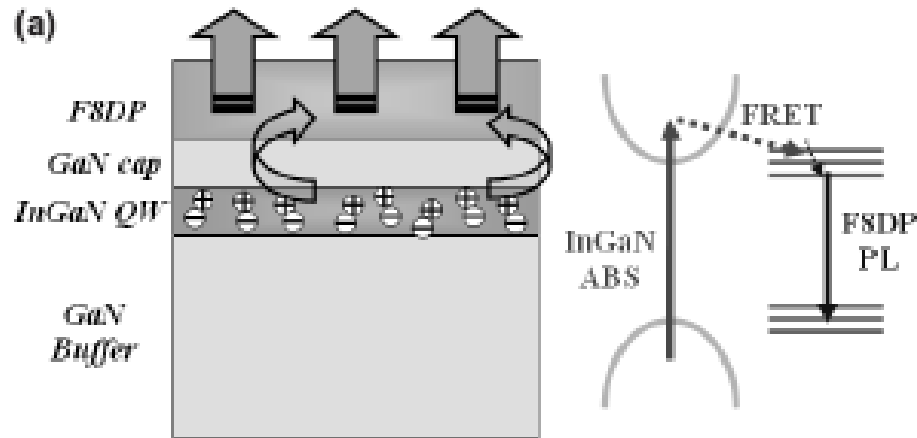
entire visible spectrum

direct electrical injection is issue

FRET can lead to higher overall luminescence efficiencies than in comparable systems involving fluorescence-based radiative energy transfer



FRET depends on dipole-dipole interactions



- *non-radiative* transfer of an excitation generated in an InGaN/GaN QW into an overlayer of LEP
- higher overall luminescence efficiencies than in comparable systems involving fluorescence-based radiative energy transfer
- characteristic range is only a few nanometres.
- GaN cap layer must be of nanometre-scale thickness <10 nm. Its thickness determines the efficiency of the FRET process



Experimental details- sample growth

- $\text{In}_x\text{Ga}_{1-x}\text{N}/\text{GaN}$ QWs with nominal $t_{\text{QW}} = 2.5$, $x = 0.075$ nm were grown by metal-organic vapour phase epitaxy on ~ 2 mm thick GaN buffer layers on (0001) sapphire substrates.
 - Sample A: $t_{\text{GaN}} = 15$ nm
 - Sample B: $t_{\text{GaN}} = 4$ nm
 - Sample C: $t_{\text{GaN}} = 2.5$ nm
- 5nm thick polymer F8DP overlayers were spin-coated from an F8DP 4 mg/mL toluene solution.

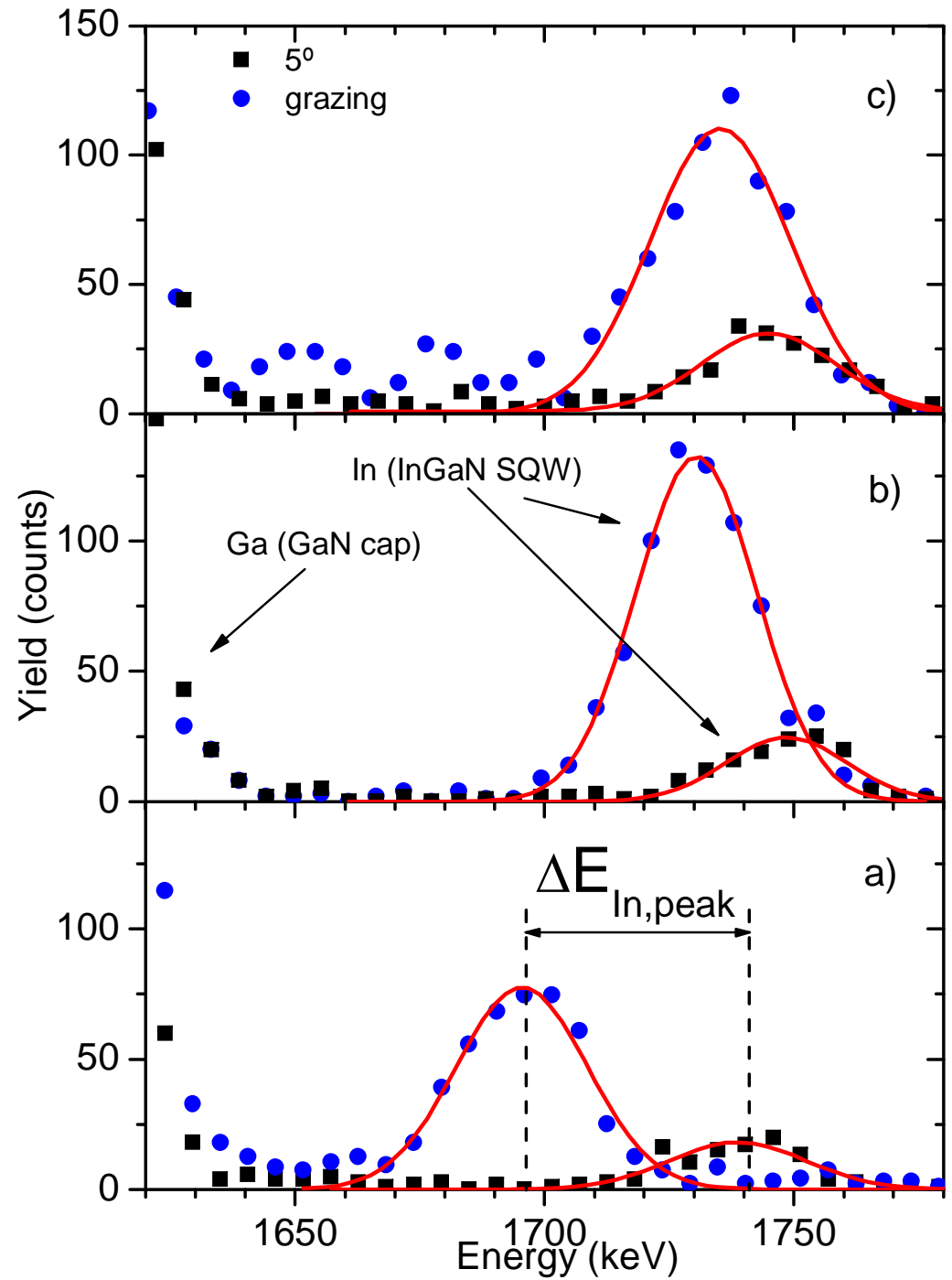
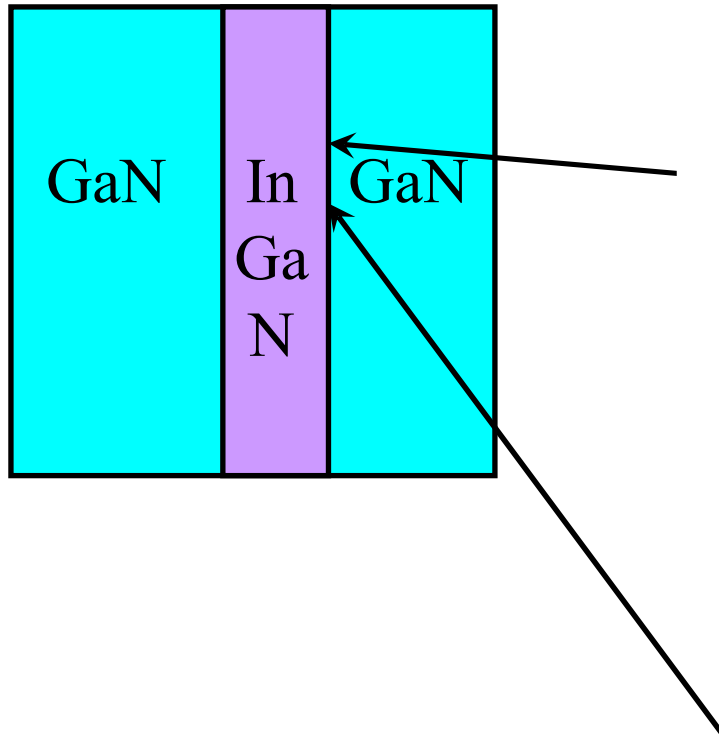


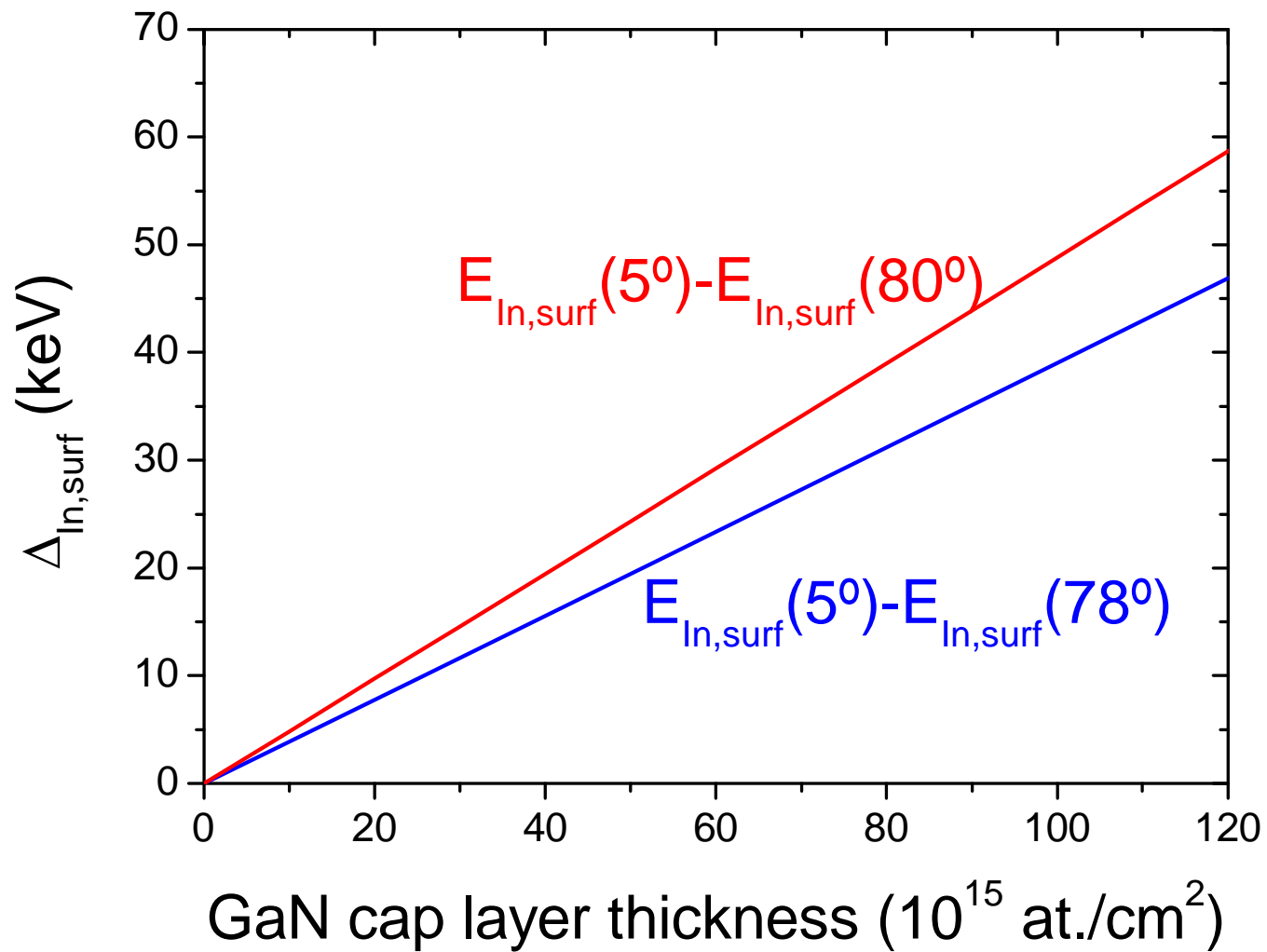
Experimental details- RBS

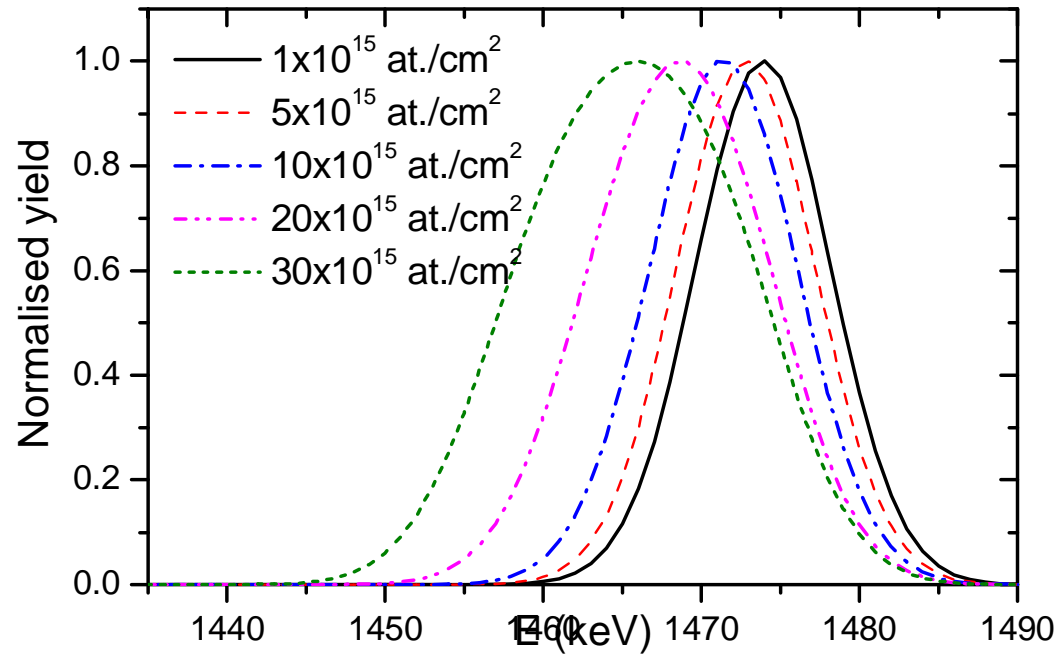
- 2.0 MeV $^4\text{He}^+$ beam detected at 160° backscattering (Cornell geometry)
- near-normal incidence (5°), and grazing angle (78° for sample A and 80° for samples B and C; the accuracy of the goniometer is 0.02°)
- beam with 0.02° angular divergence, collimated by square slits designed to reduced slit scattering, 0.6 mm high and 0.2 mm wide, leading to beam spots on the sample around 1 mm.
- The detector was located at 70 mm from the sample, and had an aperture 5 mm tall and 1.5 mm wide, to reduce the scattering angle spread.
- The beam current measured by a transmission Faraday cup with precision around 2% was kept at 2 nA.
- The pressure during the experiments was around 10^{-7} mbar.



Results

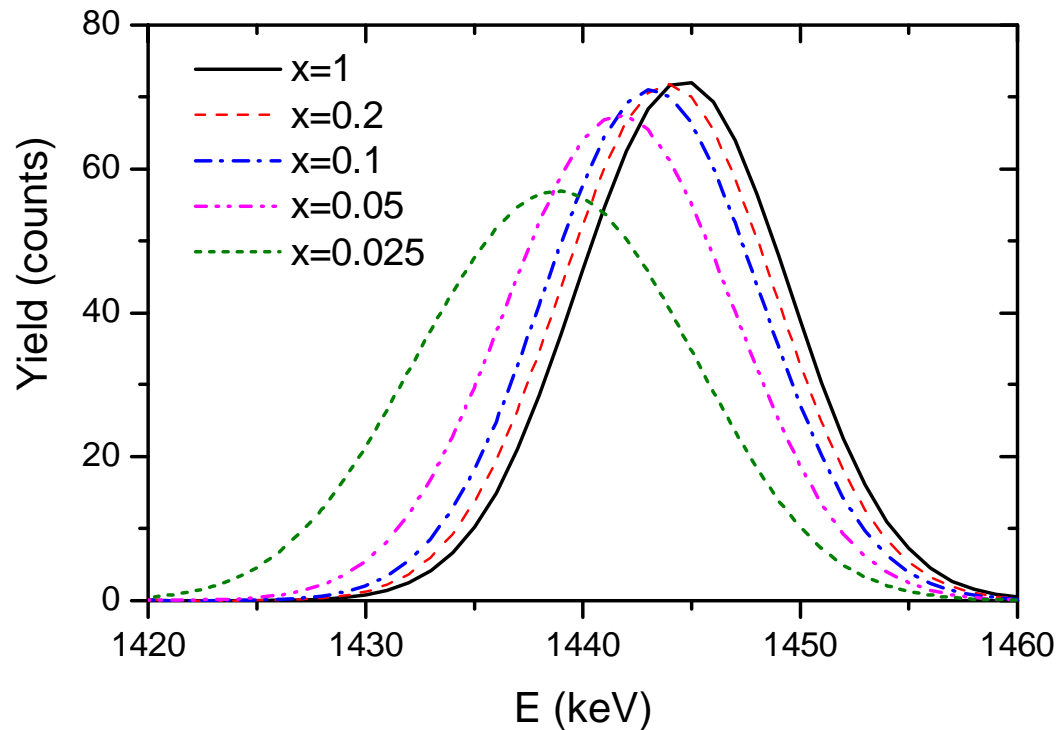






Surface pure In layers

$$E_{\text{In,surf}} \neq E_{\text{In,peak}} !!!$$



Ga_{1-x}In_xN with same In total amount, different x , below same GaN thickness



$$\Delta E_{\text{In,surf}} = E_{\text{In,surf}} (5^\circ) - E_{\text{In,surf}} (\text{grazing})$$

$$E_{\text{In,peak}} = E_{\text{In,surf}} - \Gamma_{\text{In}} / 2$$

$$\Delta E_{\text{In,surf}}(\mathbf{x}) = \Delta E_{\text{In,peak}} + \Delta \Gamma_{\text{In}}(\mathbf{x}) / 2$$

And from $\Delta E_{\text{In,surf}}(\mathbf{x})$, $t_{\text{GaN}}(\mathbf{x})$ is derived



Table 2. Results for sample A (nominally $t_{\text{GaN}} = 15$ nm). The symbols are explained in the text. The shaded lines lead to poor simulations.

x	t_{QW} (10^{15} at/cm ²)	t_{QW} (nm)	$\Gamma_{\text{In}}(5^\circ)$ (keV)	$\Gamma_{\text{In}}(78^\circ)$ (keV)	$\Delta E_{\text{In,surf}}$ (keV)	t_{GaN} (10^{15} at./cm ²)	t_{GaN} (nm)	$t_{\text{GaN}} / t_{\text{nominal}}$
0.02	50	5.7	5.16	24.91	33.41(1.03)	85.65(2.81)	9.73(30)	0.65
0.03	32	3.7	3.31	15.98	36.95(1.03)	94.67(2.81)	10.76(30)	0.72
0.05	19	2.2	1.97	9.55	39.49(1.03)	101.14(2.81)	11.49(30)	0.77
0.07	14	1.6	1.46	7.07	40.47(1.03)	103.63(2.81)	11.78(30)	0.79
0.09	11	1.1	1.16	5.59	41.07(1.03)	105.15(2.81)	11.95(30)	0.80
1	1	0.2	0.14	0.64	43.23(1.03)	110.64 (2.81)	12.57(30)	0.84



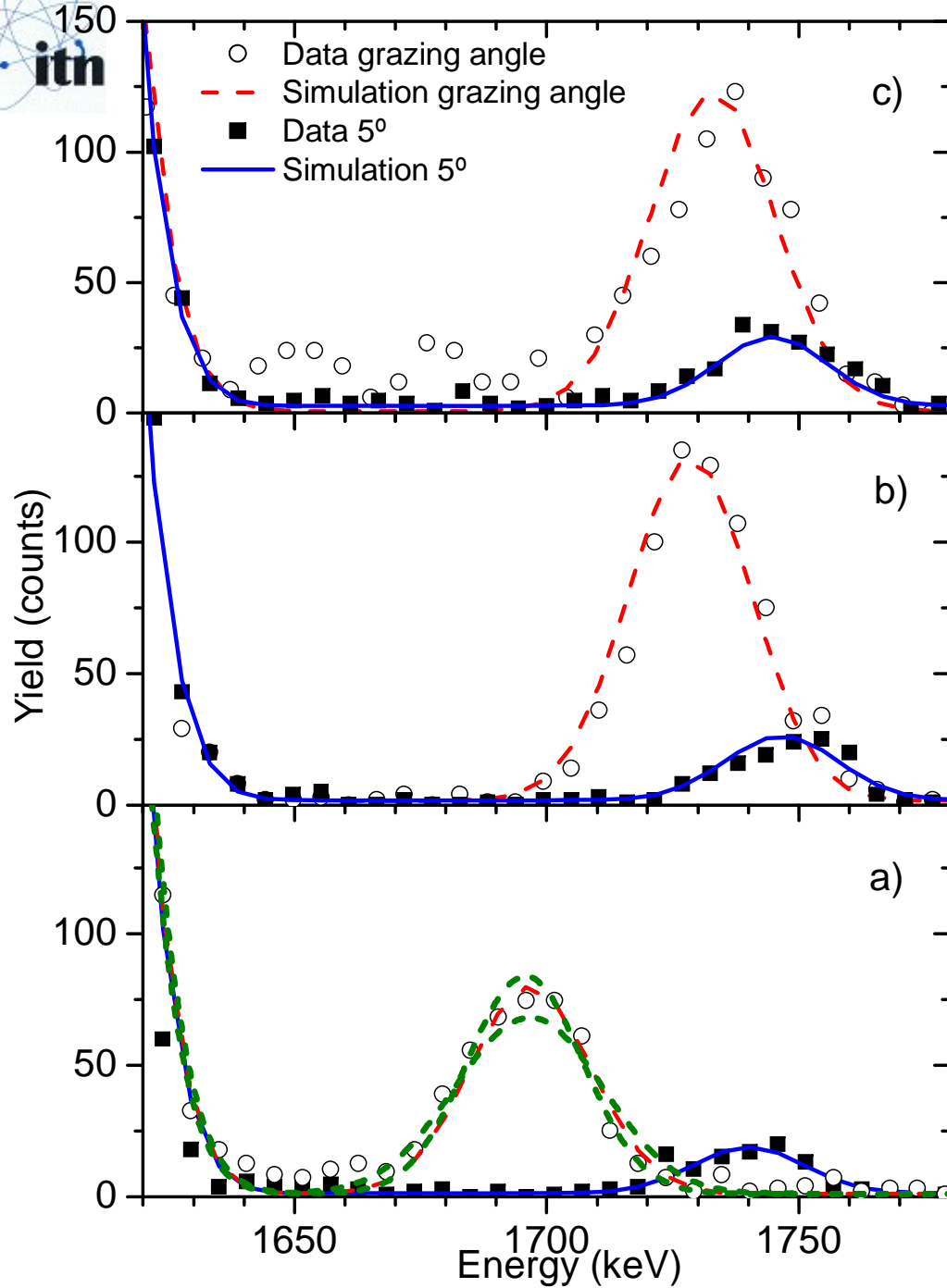
Table 3. Results for sample B (nominally $t_{\text{GaN}} = 4$ nm). The symbols are explained in the text. The shaded lines lead to poor simulations.

x	t_{QW} (10^{15} at./ cm^2)	t_{QW} (nm)	$\Gamma_{\text{In}}(5^\circ)$ (keV)	$\Gamma_{\text{In}}(80^\circ)$ (keV)	$\Delta E_{\text{In,surf}}$ (keV)	t_{GaN} (10^{15} at./ cm^2)	t_{GaN} (nm)	$t_{\text{GaN}} / t_{\text{nominal}}$
0.03	47	5.4	4.86	27.97	6.63(69)	13.65(1.42)	1.55(16)	0.39
0.05	28	3.2	2.90	16.73	11.27(69)	23.20(1.42)	2.64(16)	0.66
0.07	20	2.3	2.09	12.02	13.21(69)	27.19(1.42)	3.09(16)	0.77
0.09	16	1.9	1.64	9.40	14.30(69)	29.43 (1.42)	3.34(16)	0.83
0.11	13	1.5	1.37	7.90	14.91(69)	30.68(1.42)	3.49(16)	0.87
1	1.4	0.2	0.19	1.06	17.31(69)	35.61(1.42)	4.05(16)	1.01

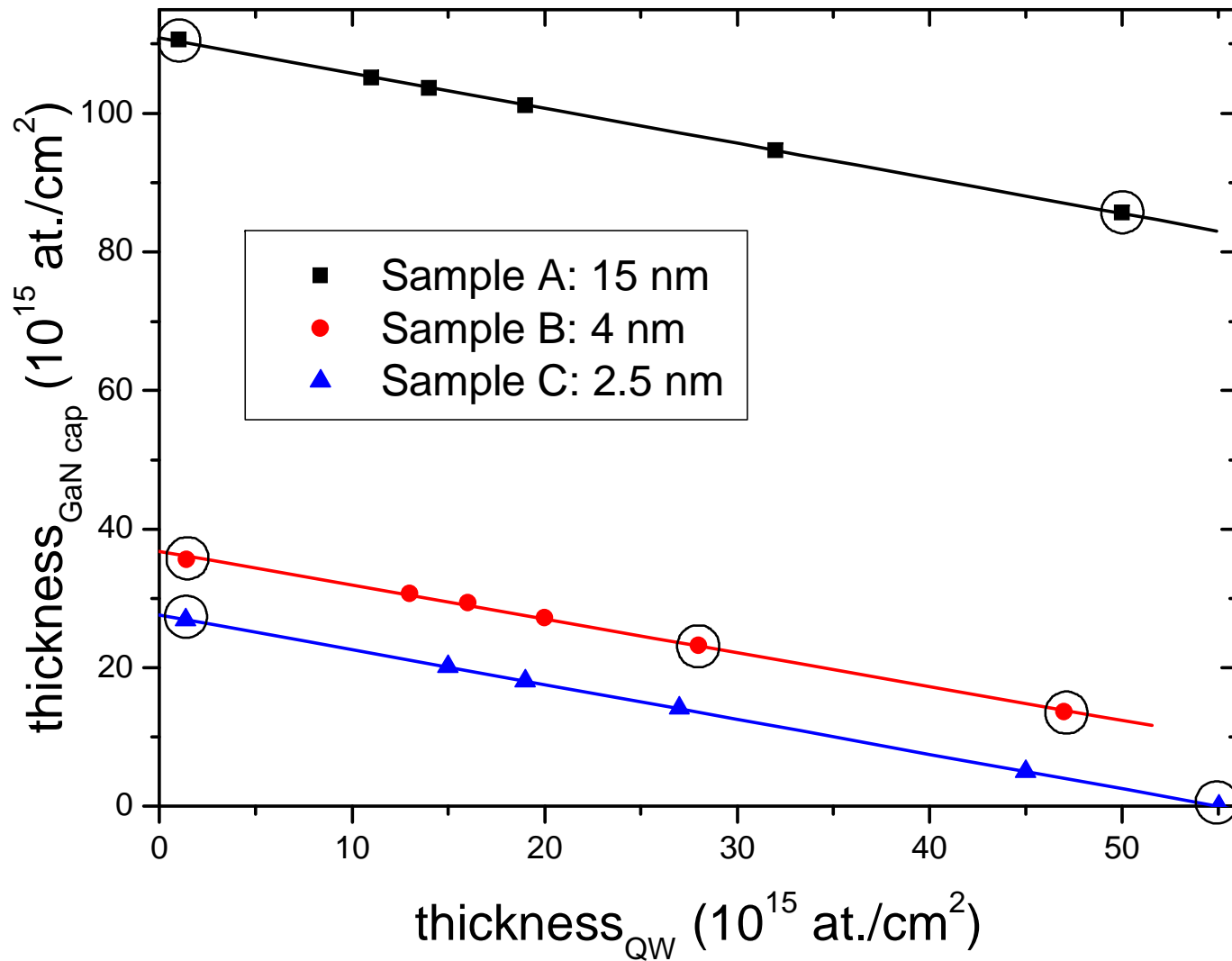


Table 4. Results for sample C (nominally $t_{\text{GaN}} = 2.5$ nm). The symbols are explained in the text. The shaded lines lead to poor simulations.

x	t_{QW} (10^{15} at./cm ²)	t_{QW} (nm)	$\Gamma_{\text{In}}(5^\circ)$ (keV)	$\Gamma_{\text{In}}(80^\circ)$ (keV)	$\Delta E_{\text{In,surf}}$ (keV)	t_{GaN} (10^{15} at./cm ²)	t_{GaN} (nm)	$t_{\text{GaN}} / t_{\text{nominal}}$
0.025	55	6.3	5.67	32.65	0(1.01)	0(2.06)	0(0.23)	0
0.03	45	5.1	4.65	26.74	2.45(1.01)	4.95(2.06)	0.56(23)	0.22
0.05	27	3.1	2.81	16.12	6.85(1.01)	14.11(2.06)	1.60(23)	0.64
0.07	19	2.2	1.98	11.40	8.79(1.01)	18.11(2.06)	2.06(23)	0.82
0.09	15	1.7	1.58	9.06	9.76(1.01)	20.10 (2.06)	2.28(23)	0.91
1	1.35	0.2	0.17	1.02	13.07(1.01)	26.90(2.06)	3.06(23)	1.22



Some solutions rejected due to wrong width of In peak



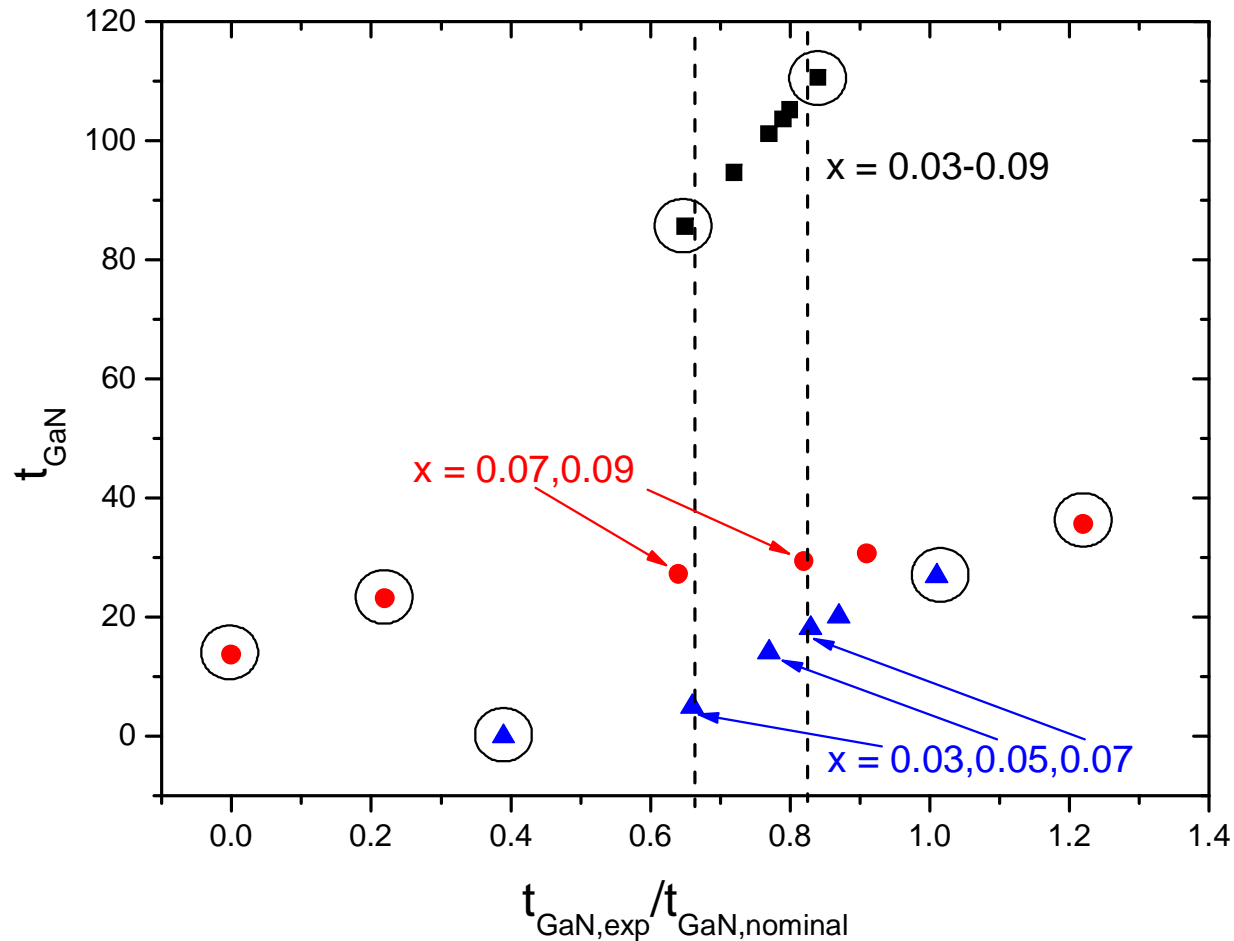
$$t_{\text{GaN}} = -t_{\text{QW}}/2 + \Delta E_{\text{In,peak}} / S(1/\cos(\text{grazing}) - 1/\cos(5^\circ)) (k - 1/\cos(\pi - \alpha_{\text{scatt}}))$$



All QWs grown in exactly the same way

Control and reproducibility of growth excellent

- x must be the same in all samples
- $t_{\text{GaN,exp}}/t_{\text{GaN,nominal}}$ must be the same in all samples

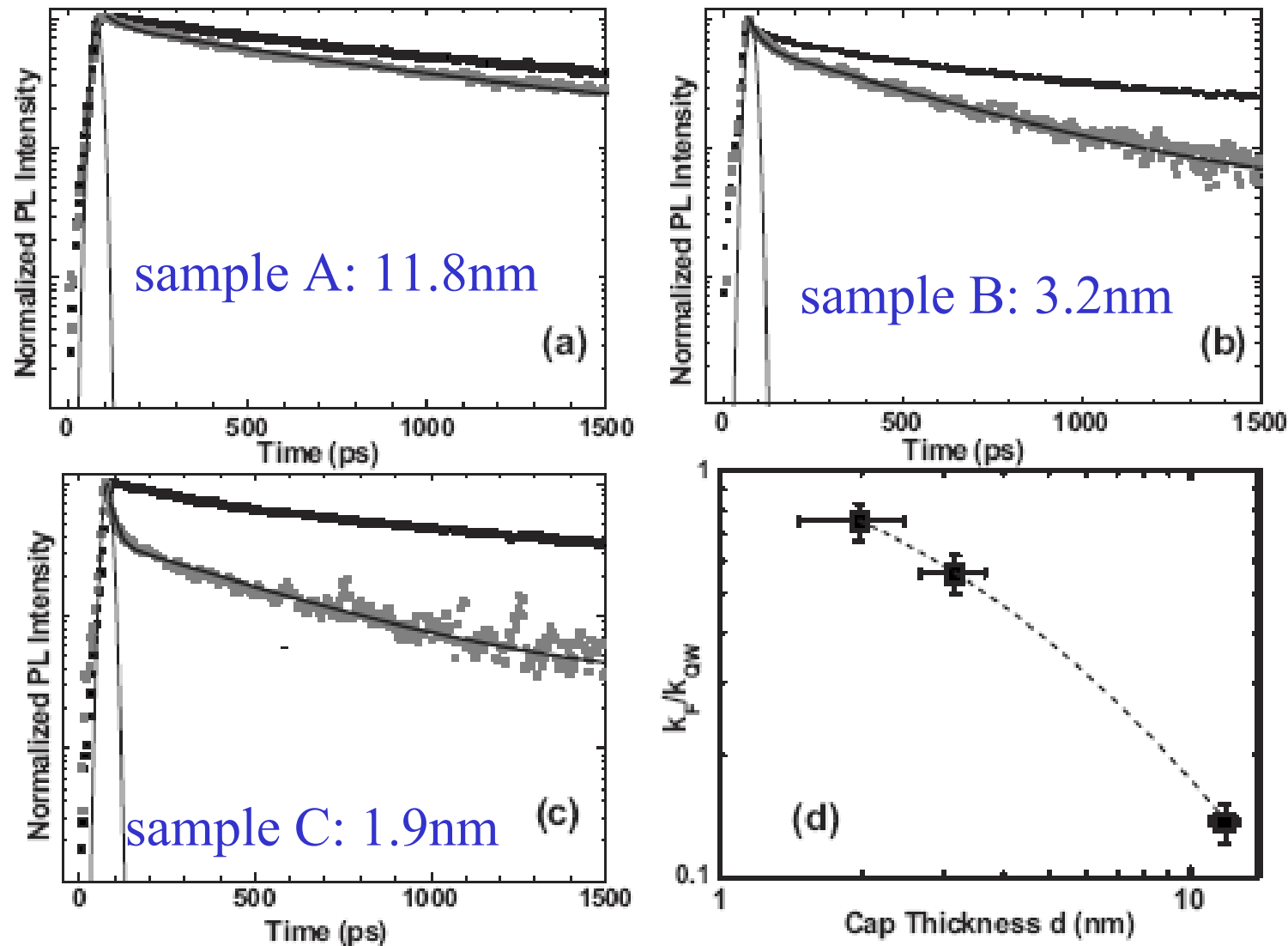


$$x=0.07(1), \quad t_{\text{GaN,exp}}/t_{\text{GaN,nominal}}=0.79(5), \quad t_{\text{QW}} = 2.0(4)\text{nm}$$

**GaN cap layer thickness of samples A, B and C:
11.8(8) nm, 3.2(5) nm, 1.9(5) nm**



PL at QW peak with and without LEP



Förster radius: 6.1(0.8) nm typical for 2D-2D FRET; efficiency at LN: 60%



Conclusions

- Do not trust data analysis codes
 - Good fits are meaningless when data are ambiguous
- Learn how to do manual analysis
 - Sometimes it's the only way of doing things right
- Analysis codes are nevertheless essential
 - They make your life much easier